Vietnam Journal of Science and Technology ***62*** *(2024)*

doi:10.15625/2525-2518/18511

Effect of rice husk morphology on the ability to synthesize silicon carbide by pyrolysis method

Kieu Do Trung Kiem[1, 2, *], Ong Dieu Hanh[1, 2], Nguyen Hoang Thien Khoi[1, 2], Huynh Ngoc Minh

[1]*Faculty of Materials Technology, Ho Chi Minh City University of Technology (HCMUT), 268 Ly Thuong Kiet Street, District 10, Ho Chi Minh City, Viet Nam*

[2]*Vietnam National University Ho Chi Minh City, Linh Trung Ward, Thu Duc City, Ho Chi Minh City, Viet Nam*

[*]Emails: *kieudotrungkien@hcmut.edu.vn*

Received: 13 July 2023; Accepted for publication: 8 July 2024

Abstract. Silicon carbide (SiC) is a mineral with good technical properties and high economic value. However, the synthesis of SiC is expensive because it is synthesized at a high-temperature environment (above 1500 ^{o}C). The synthesis of SiC from biomass can significantly reduce the synthesis temperature. One commonly used biomass material for synthesizing SiC is rice husk. However, the ability to synthesize SiC depends on the shape of the rice husk. The influence of the morphology of rice husk on the ability to synthesize SiC was studied in this study. Experimental results showed that the original rice husk would give better SiC formation capacity than the rice husk powder. The amount of SiC formed using the original rice husk when impregnated by sodium silicate solution and pyrolysis at 1200 ^{o}C is 18.3 % (wt%.). With rice husk powder, it is 15.12 % (wt%.). The results of analysis of the mineral composition, functional groups, and morphologies by X-ray diffraction (XRD), Fourier Infrared Transform Method (FT-IR), and Scanning Electron Microscopy (SEM) found that the polymorphy of SiC is α-SiC and β-SiC. These minerals are the basis for SiC from rice husks, which can be applied as wear-resistant materials.

Keywords: silicon carbide, rice husk, pyrolysis, SiC/SiO_2/C composite

Classification numbers: 3.4.3, 2.9.4, 2.10.2.

1. INTRODUCTION

Silicon Carbide is a mineral with the main composition of silicon (Si) and carbon (C). It is a material with the chemical formula. Silicon Carbide is a new material widely used in many fields thanks to its unique properties. SiC usually exists as small particles, thin sheets, or large plates. It is black and can have a hardness comparable to a diamond.

SiC has a larger band gap than traditional silicon (Si) semiconductors. Therefore, SiC is a very potential semiconductor material [1]. Due to its large bandgap energy, it can withstand stronger electric fields, high operating temperatures, and higher voltage increases than silicon.

SiC could become an ideal material for high-power electronic applications. Silicon Carbide is used to fabricate power electronic components such as motor control circuits, inverters, voltage stabilizers, and industrial electrical cabinets [2, 3]. Its high voltage and heat resistance helps increase efficiency and reduce the size of power electronic systems [4]. SiC can fabricate blue, green, and white LEDs [5, 6]. SiC LED has high brightness, long life, and energy saving compared to traditional LEDs [7]. In addition, SiC is used in power conversion and control devices, including applications such as solar inverters, electric vehicles, and electrical systems in aircraft, ships, and hybrid cars [8, 9].

Besides potential applications in the fields of electricity and electronics, SiC can also be applied as mechanical and heat-resistant materials thanks to its mechanical strength and high temperature resistance. SiC has been used in the production of mechanical parts that require high hardness, high temperature resistance, and wear resistance [10, 11]. Applications include wear-resistant machinery parts, bearings, transmissions, and heat-resistant parts. SiC has good heat resistance, so it is used in highly heat-resistant applications such as refractories, insulation materials, heat resistant pipes, and components in furnaces, boilers, and heating systems [12]. SiC is used in the automotive industry to enhance critical components' hardness and wear resistance, such as brakes, bearings, valves, and pistons [13]. SiC can also be used in applications to improve engine performance and reduce weight [14]. In addition to being the primary raw material, SiC can also act as an additive to synthesize materials. SiC can be considered a foaming additive in ceramic products. When heating SiC in an O_2 atmosphere, SiC will form CO_2 gas and contribute to the foaming of ceramic products [15]. Carbon produced during the decomposition of SiC can also be used as an additive in the production of Cr_2AlC [16]. Cr_2AlC is a potential compound in photocatalytic applications.

The above properties and applications show the role and potential of SiC materials. Currently, in industry, SiC materials are usually made through a chemical reaction between compounds containing carbon (C) and silicon (Si). Commonly used materials for this synthesis are SiO_2 and C powder. The temperature to synthesize SiC is above 1500 ^oC [17].

With the traditional method, SiC is usually formed at other high temperatures (above 1500 ^oC). Therefore, the synthesis of SiC is quite tricky, so the cost of this material is increased. To solve this problem, many research groups have studied the preparation of SiC from biomass sources. Synthesis of SiC from biomass materials can produce SiC at temperatures above 700 ^oC [18]. As a result, SiC production costs will be lower. SiC materials may be more commonly used in civil applications. Creating SiC from biomass is also one of the methods that can be applied to treat agricultural wastes. M. Khangkhamano et al. have studied the fabrication of SiC from bagasse. Bagasse has been pulverized and reacted with silicon at high temperatures. As a result of the study, SiC was formed at a temperature of 1800 ^oC [19]. SiC can also be synthesized from sawdust. Using the same method, V. C. Bringas-Rodriguez et al. also obtained SiC from sawdust at 500 ^oC [20]. In the studies on SiC fabrication from biomass materials, rice husk is commonly used [18]. With the characteristic that rice husk contains a lot of silicon and carbon, this is a suitable source of raw materials to create SiC.

However, few studies on rice husk mention the ability to form SiC when using rice husk material with different morphology. In this study, we fabricated SiC from crushed and original rice husks. By analytical methods such as chemical composition, X-ray diffraction, Fourier transform infrared spectroscopy, and scanning electron microscopy, the ability to form SiC was investigated. The obtained results provide information on the influence of rice husk morphology on the ability to synthesize SiC.

2. MATERIALS AND METHODS

Rice husk material (RH) is taken from Long An province - Vietnam. The chemical composition of rice husks was determined by X-ray Fluorescence and Isotope Ratio Mass Spectrometry methods. The results are presented in Table 1. Rice husks were washed and dried at 90 ^{o}C for 24 hours. After drying, the husks were divided into two groups. Group 1 (symbol G1) was preserved with the original rice husk. Group 2 (symbol G2) was milled in a crushing machine. The average particle size of group 2 is 47.71 µm. The particle size distribution of group 2 is shown in Figure 1. Sodium silicate ($Na_2SiO_3.nH_2O$ – symbol SS) was also used to add the silicon component. The density and module of sodium silicate are 1.5 g/ml and 2.9.

Table 1. Chemical composition (% wt.) of RH.

C	N	H	Si	Fe	Mg	Na	K	Al	P	S	Mn	Othes
45.91	3.12	6.12	8.38	0.38	0.05	0.09	0.18	0.09	0.11	0.01	0.02	35.53

SiO_2	Na_2O	K_2O	Fe_2O_3	Al_2O_3	LOI	Others
6.71	0.38	0.23	0.19	0.15	92.13	0.12

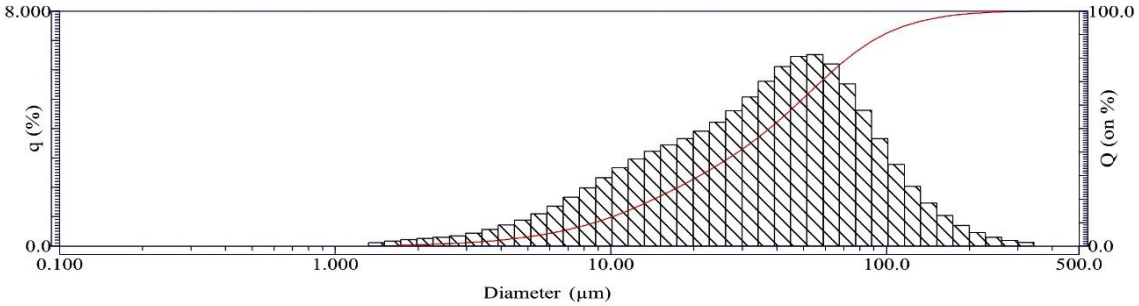

Figure 1. The particle size distribution of the crushed rice husks.

Two groups of RH were soaked in SS solution at the ratio of 5g rice husk/ 1 liter of SS. The soaking time of RH was 24 hours. After 24 hours, SS would adhere to the surface of the rice husk. Thanks to that, the RH would be supplied with Si for the SiC generation reaction. RH and SS mixtures were dried at different temperatures until the weight remained constant. After drying, the mixtures were sintered at 1200 ^{o}C in a prevent oxygen environment with a heating rate of 10 ^{o}C/min. Finally, the sintered samples were analyzed for properties such as the formed SiC content, microstructure, and mineral composition to evaluate the reactivity to generate SiC of 2 groups of materials.

The sintered powders were milled to a particle size of less than 150 µm. Samples were taken according to ISO 5022 standards. The SiC content in the product was determined according to ISO 21068:2008 standards. The functional group was analyzed by Fourier transform infrared spectroscopy (FT-IR). Scanning ranges are 450 - 4000 cm^{-1}. The scan step is 0.96425 cm^{-1}. The mineral composition was analyzed by X-ray diffraction (XRD). Samples were measured at 2θ from 5 to 70º with a scan step of 0.019º. The microstructure was evaluated by scanning electron microscopy (SEM).

3. RESULTS AND DISCUSSION

RH is the source of Si and C for the SiC generation reaction. T. D. Dinh et al. have shown that RH can be a source of raw materials to provide SiO_2 [21]. However, the Si content in RH is low. It is necessary to add materials to provide Si components. In this study, SS is the raw material to provide Si. In addition, SS also contains the sodium element. In many studies, sodium has been shown as one of the ingredients that can act as an additive to promote SiC generation. Sodium acts as an early liquid phase-forming agent. Thanks to the surface tension of this liquid phase, the crystallization process of SiC takes place more easily. Therefore, more SiC can be formed at lower temperatures. RH (solid phase) is mixed with SS (liquid phase) by impregnation. Figure 2 is the result of determining the adhesion ability of SS on the RH surface in two groups of RH particles at different drying temperatures.

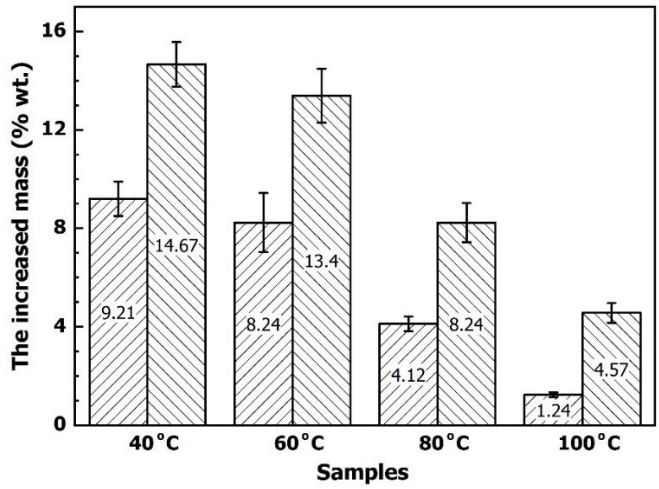

Figure 2. The mass increase of RH material groups after soaking (% wt.)

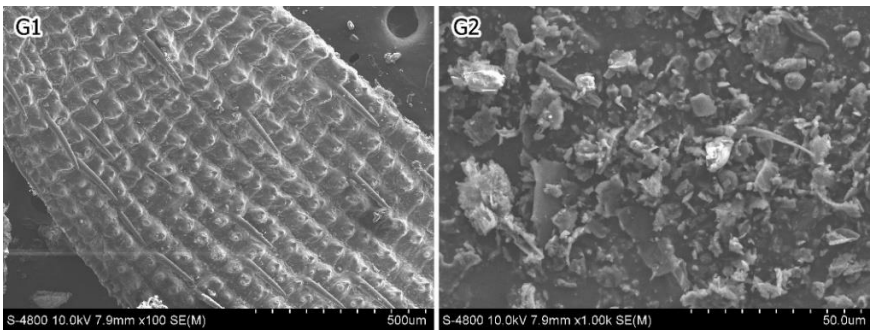

Figure 3. The SEM images of RH of group 1 (G1) and group 2 (G2).

The results of Figure 2 also show a significant mass difference between the G1 and G2 groups. Considering the same drying temperature, the G1 sample with a large particle size gained less mass than the G2 sample. The results show that the particle size affects the ability to retain SS. The smaller the particle size of the material, the greater the ability to keep SS. In this case, the ability to keep SS is related to the surface area of the material. Observing the SEM image in Figure 3, the G2 sample has a grain size many times smaller than the G1 sample. If the material has a small particle size, the surface area of the material will increase. As the area exposed to SS increases, the ability to retain SS also increases. The ability to hold SS also

contributes to an increase in the amount of Si for the G2 sample. Therefore, the G2 sample is expected to form a lot of SiC after calcination.

When comparing different drying temperatures, the results of Figure 2 show that the higher the drying temperature, the lower the amount of SS kept. As the drying temperature increases, the drying speed will also increase. SS components will be swept away by water evaporation. Therefore, the amount of SS retained in the RH decreases.

The G1 and G2 samples, after being impregnated with SS and dried at different temperatures (40, 60, 80, and 100 ^{o}C), would be sintered at 1200^{o}C to synthesize SiC. The sintered G1 and G2 samples were analyzed to determine the amount of SiC formed. Figure 4 is the result of determining SiC content according to ISO 21068:2008 standards.

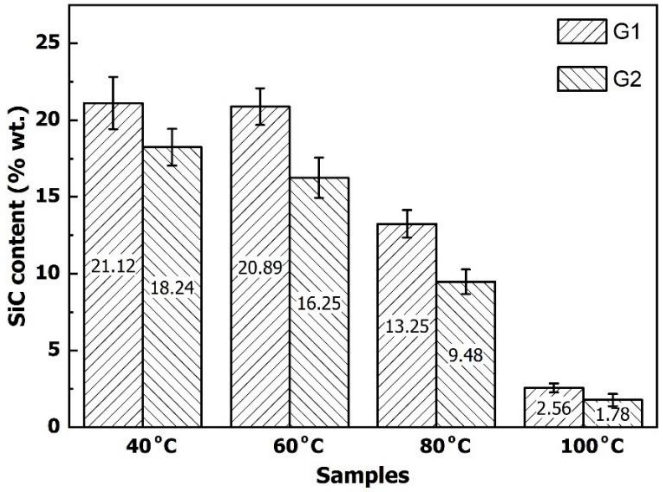

Figure 4. The SiC content of G1 and G2 samples after sintered at 1200 ^{o}C (% wt).

The results of Figure 4 show that SiC was synthesized when the samples were sintered at 1200 ^{o}C. The results of SiC content decreasing with increasing drying temperature in Figure 4 show the role of SS in the process of SiC generation. As the drying temperature increased, the amount of SS kept on the RH surface decreased (Figure 3). The Si composition in the system also reduces, so the amount of formed SiC during the heating process also decreases.

Considering the two groups of particles, the results of Figure 4 contrast the results of Figure 3. In Figure 3, the G2 group with a small particle size and large surface area should keep a lot of SS during the impregnation process. Theoretically, with the increase of SS, the content of SiC in the G2 group will also be higher than in the G1 group. However, experiments have shown the opposite results. The G1 group materials showed higher SiC content than the G2 group in all samples. Some previous studies have demonstrated that the SiC generation reaction will be reduced when the CO_x content in the system increases [22, 23]. The mechanism of SiC formation is shown in chemical equation from (1) to (5). As the CO_x content increases, the balance of the chemical reaction that produces SiC will shift to the left of (1), (4), and (5) reactions. So, the SiC content will also decrease. In this case, the space between the particles increases because the G1 group has a larger particle size than the G2 group. The CO_x formed during the pyrolysis of RH was quickly released. Since then, the CO_x content in the system has also been reduced. It helps SiC to create more.

$$SiO_2\ (s) + 3C\ (s) \rightarrow SiC\ (s) + 2CO\ (g) \quad (1)$$

$$SiO_2\ (s) + C\ (s) \rightarrow SiO\ (g) + CO\ (g) \quad (2)$$

$$SiO_2\ (s) + CO\ (g) \rightarrow SiO\ (g) + CO_2\ (g) \quad (3)$$

$$SiO\ (g) + 2C\ (s) \rightarrow SiC\ (s) + CO\ (g) \quad (4)$$

$$SiO\ (g) + 3CO\ (g) \rightarrow SiC\ (s) + 2CO_2\ (g) \quad (5)$$

Figure 3 and Figure 4 show that the G1 sample with high ventilation gives a higher SiC content than the G2 sample under the same synthesis conditions. In addition, 40 ^oC and 60 ^oC are suitable temperatures for drying SS and RH. However, 40 ^oC will give more drying time than 60 ^oC. Therefore, 60 ^oC is chosen for drying the SS and RH. Samples of the sintered G1 and G2 group at 1200 ^oC will be analyzed by FTIR and XRD to analyze the composition of mineral composition. Figure 5 is the result of the FTIR analysis, and Figure 6 is the result of the XRD patterns.

The FT-IR results in Figure 5 are typical for SiC products synthesized from biomass sources. The vibration at 3100 – 3600 cm^{-1} on the FT-IR spectrum is characteristic of the O-H group [24]. The O-H group represents the moisture in the samples—the vibration characteristic for the Si-C covalent bond at position 789 cm^{-1} [24]. In addition, because the precursor is a source of biomass, the product will contain C=O, C=C groups at the position of wavenumber 1720, 1632 cm^{-1} [25]. The vibrations of the Si-O, Si-O-Si bonds at 1059, 812, and 464 cm^{-1} [24, 26] are typical for the Si component that does not react entirely and is oxidized to SiO_2 afterward. From the FT-IR results, there was a formation of SiC at 1200 ^oC in both the G1 and G2 groups. However, the formed SiC contains many impurities. Impurities formed after sintering are typical by-products of SiC synthesis from biomass sources [27]. SiC made from biomass sources can be used in applications with low SiC purity. If some chemical and thermal methods remove other components, such as C and SiO_2, pure SiC can be completely formed from rice husks.

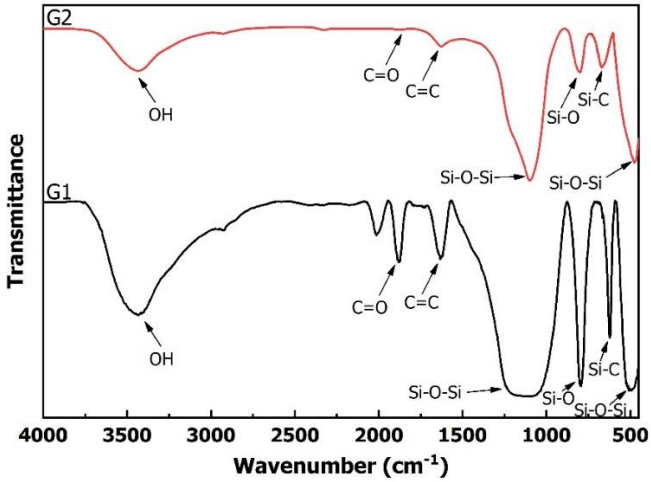

Figure 5. The FTIR spectrum of G1 and G2 samples after sintered at 1200 ^oC.

The XRD method was also used to determine the mineral composition of the G1 and G2 groups after sintering (Figure 6). The samples' XRD pattern after sintering shows the similarity in mineral composition. The XRD results also confirmed the mineral composition of the product as indicated in the FTIR spectrum. In the G1 and G2 samples, minerals, including cristobalite (SiO_2), α-SiC, and β-SiC, were formed after sintering. The mineral cristobalite (JCPDS card No. 39-1425) is represented at the 21.99^o, 36.5^o, and 54.2^o diffraction positions [28]. Cristobalite is

the high temperature polymorph of SiO_2. It is formed by heating SiO_2 without a catalyst [29]. Mineral β-SiC (JCPDS card No. 29-1129) is present at 35.6°, 41.6°, and 60° diffraction positions [24]. β-SiC is a low-temperature polymorph of SiC. This is a common mineral that occurs with low-temperature SiC synthesis methods. It is also a transition mineral before the formation of α-SiC. The α-SiC mineral (JCPDS card No. 01-073-1664) is represented at the 34.1°, 38°, and 66.5° diffraction position [24]. α-SiC is the high-temperature polymorph of SiC. Previous studies showed that α-SiC usually forms at sintered temperatures above 1500 °C. This result indicates that it is possible to create different SiC polymorphs at low temperatures by sintered RH impregnated with SS.

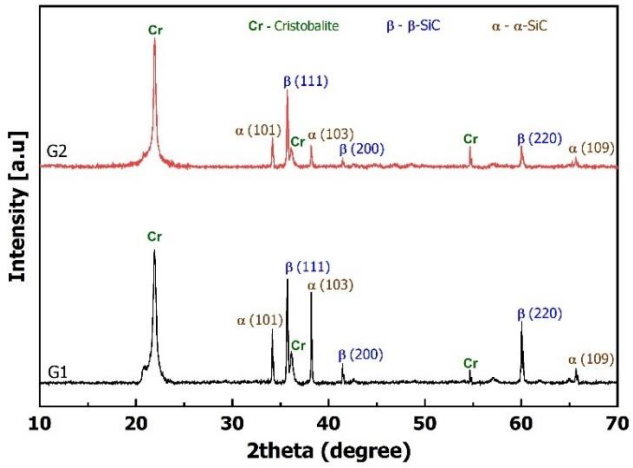

Figure 6. The XRD patterns of G1 and G2 samples after sintered at 1200°C.

In addition to forming similar minerals in the G1 and G2 groups, the XRD patterns of the two samples also show the difference in the intensity of the peaks related to SiC minerals. This difference is easily observed when comparing the intensity ratio of the SiC peaks to the cristobalite peaks. The results show that the intensity of SiC peaks in the G1 sample is higher than in the G2 sample. It proves that SiC crystals in the G1 sample grow better than in the G2. This observation again proves that the formation of SiC minerals in the G1 sample is more favorable than in the G2 sample. The reason for this advantage is that the ventilated form of the G1 model allows CO_x to escape quickly.

4. CONCLUSIONS

In this study, SiC was made from RH impregnated with SS and sintered at 1200 °C. The analysis results of SS keeping capacity, chemical composition, functional group, and mineral composition also showed the ability to create SiC of two groups of raw materials, original RH (G1 group) and crushed RH (G2 group). The G2 group with small particle size and large surface area will be better able to keep SS during RH impregnation with SS. However, the G1 group with good ventilation will help the CO_x formed during the pyrolysis to release quickly. As a result, the balance of the chemical equation for the formation of SiC will shift from left to right. The content of SiC of the G1 sample is formed more than the G2 sample. The formed SiC has two polymorphs, including β-SiC and α-SiC. They are two low- and high-temperature polymorphs of SiC. In addition, there is also the presence of cristobalite (SiO_2) and carbon in the composition of the samples after sintering. They are products that form when the C and Si

precursors react uncompletely. Therefore, SiC synthesized from biomass can be used in applications without high purity. This can also be a precursor to forming pure SiC through C and SiO_2 reduction processes.

Acknowledgements. This research is funded by Vietnam National University Ho Chi Minh City (VNU-HCM) under grant number: B2023-20-18. We acknowledge Ho Chi Minh City University of Technology (HCMUT), VNU-HCM for supporting this study.

CRediT authorship contribution statement. Kieu Do Trung Kien: Methodology, Funding acquisition. Ong Dieu Hanh: Formal analysis. Nguyen Hoang Thien Khoi: Formal analysis. Huynh Ngoc Minh: Investigation, Supervision.

Declaration of competing interest. The authors declare that they have no known competing financial interests or personal relationships that could have appeared to influence the work reported in this paper.

REFERENCES

1. Neudeck P. G. - Progress in silicon carbide semiconductor electronics technology, J. Electron. Mater. **24** (1995) 283-288. https://doi.org/10.1007/BF02659688
2. Kong X., Nie R., and Yuan J. - Shape stabilized three-dimensional porous SiC-based phase change materials for thermal management of electronic components, Chem. Eng. J. **462** (2023) 142168. https://doi.org/10.1016/j.cej.2023.142168
3. Singh S., Chaudhary T., and Khanna G. - Recent advancements in wide band semiconductors (SiC and GaN) technology for future devices, Silicon **14** (11) (2022) 5793-5800, 2022. https://doi.org/10.1007/s12633-021-01362-3
4. Alves L. F. S, Gomes R. C. M., Lefranc P., Pegado R. D. A., Jeannin P. O. Luciano B. A., and Rocha F. V. - SIC power devices in power electronics: An overview, Brazilian Power Electronics Conference (COBEP), Barzil, 2017, pp. 1-8. https://doi.org/10.1109/COBEP.2017.8257396
5. Edmond J. A., Kong H. S., and Carter Jr C. H. - Blue LEDs, UV photodiodes and high-temperature rectifiers in 6H-SiC, Phys. B (Amsterdam, Neth.) **185** (1-4) (1993) 453-460. https://doi.org/10.1016/0921-4526(93)90277-D
6. Feng D. H., Jia T. Q., Li X. X., Xu Z. Z., Chen J., Deng S. Z., Wu Z. S., and Xu N. S. - Catalytic synthesis and photoluminescence of needle-shaped 3C–SiC nanowires, Solid State Commun. **128** (8) (2003) 295-297. https://doi.org/10.1016/j.ssc.2003.08.025
7. J. Edmond J., Abare A., Berman M., Bharathan J., Bunker K. L., Emerson D., Haberern K., Ibbetson J., Leung M., Russel P., and Slater D. - High efficiency GaN-based LEDs and lasers on SiC, J. Cryst. Growth **272** (1-4) (2004) 242-250. https://doi.org/10.1016/j.jcrysgro.2004.08.056
8. Ni Z., Lyu X., Yadav O. P., Singh B. N., Zheng S., and Cao D. - Overview of real-time lifetime prediction and extension for SiC power converters, IEEE T. Power Electr. **35** (8) (2019) 7765-7794. https://doi.org/10.1109/TPEL.2019.2962503
9. Louro P., Vieira M., Fernandes M., Costa J., Vieira M. A., Caeiro J., Neves N., and Barata M. - Optical demultiplexer based on an a-SiC: H voltage controlled device, Phys. Status Solidi C **7** (3-4) (2010) 1188-1191. https://doi.org/10.1002/pssc.200982702

10. Prasad K. E. and Ramesh K. - Hardness and mechanical anisotropy of hexagonal SiC single crystal polytypes, J. Alloys Compd. **770** (2019) 158-165. https://doi.org/10.1016/j.jallcom.2018.08.102
11. Su L., Wang H., Niu M., Fan X., Ma M., Shi Z., and GUo S. W. - Ultralight, recoverable, and high-temperature-resistant SiC nanowire aerogel, ACS nano **12** (4) (2018) 3103-3111. https://doi.org/10.1021/acsnano.7b08577
12. Wang H. F., Bi Y. B., Zhou N. S., and Zhang H. J. - Preparation and strength of SiC refractories within situ β-SiC whiskers as bonding phase, Ceram. Int. **42** (1) (2016) 727-733. https://doi.org/10.1016/j.ceramint.2015.08.172
13. Borrero-López O., Ortiz A. L., Guiberteau F. , and Padture N. P. - Microstructural design of sliding-wear-resistant liquid-phase-sintered SiC: an overview, J. Eur. Ceram. Soc. **27** (11) (2007) 3351-3357. https://doi.org/10.1016/j.jeurceramsoc.2007.02.190
14. Spitsberg I. and Steibel J. - Thermal and environmental barrier coatings for SiC/SiC CMCs in aircraft engine applications, Int. J. Appl. Ceram. Technol. **1** (4) (2004) 291-301. https://doi.org/10.1111/j.1744-7402.2004.tb00181.x
15. Kien K. D. T., Thuy D. D. X., Nhi N. V. U., and Minh D. Q. - The formation of red copper Glaze in an Oxidizing Atmosphere, Iran. J. Mater. Sci. Eng. **20** (3) (2023) 1-9. https://doi.org/10.22068/ijmse.3141
16. Ta Q. T. H., Tran, N. M., and Noh J. S. - Pressureless manufacturing of Cr_2AlC compound and the temperature effect, Mater. Manuf. Processes **36** (2) (2021) 200-208. https://doi.org/10.1080/10426914.2020.1819547
17. Krishnarao R., Godkhindi M., Chakraborty M., and Mukunda P. - Formation of SiC whiskers from compacts of raw rice husks, J. Mater. Sci. **29** (1994) 2741-2744. https://doi.org/10.1007/BF00356826
18. Khai T. V., Minh H. N., Nhi N. V. U., and Kien K. D. T. - Effect of composition on the ability to form SiC/SiO_2-C composite from rice husk and silica gel, J. Ceram. Process. Res. **22** (2) (2021) 246-251. https://doi.org/10.36410/jcpr.2021.22.2.246
19. Khangkhamano M., Singsarothai S., Kokoo R., and Niyomwas S. - Conversion of bagasse ash waste to nanosized SiC powder, Int. J. Self-Propag. High-Temp. Synth. **27** (2018) 98-102. https://doi.org/10.3103/S1061386218020103
20. Bringas-Rodríguez V., Huamán-Mamani F., Paredes-Paz J., and Gamarra-Delgado J. - Evaluation of thermomechanical behavior in controlled atmospheres of silicon carbide obtained from sawdust residues of the Peruvian timber industry, Mater. Today: Proc. **33** (2020) 1835-1839. https://doi.org/10.1016/j.matpr.2020.05.175
21. Dinh T. D., Nguyen Q. L., Vu M. D., Tran T. M. H., Tran T. H. N, Nguyen M. H., and Pham T. D. - Adsorption characteristics of Cu2+ on CeO2/SiO2 nanomaterials based on rice husk and its application to pre-concentration and determination in food samples, Colloid Polym. Sci. (2023). https://doi.org/10.1007/s00396-023-05140-y
22. Wang Y., Zhang L., Zhang X., Zhang Z., Tong Y., Li F., Wu J. C. S., and Wang X. - Openmouthed β-SiC hollow-sphere with highly photocatalytic activity for reduction of CO_2 with H_2O, Appl. Catal. B **206** (2017) 158-167. https://doi.org/10.1016/j.apcatb.2017.01.028

23. Goto T. and Homma H. - High-temperature active/passive oxidation and bubble formation of CVD SiC in O_2 and CO_2 atmospheres, J. Eur. Ceram. Soc. **22** (14-15) (2022) 2749-2756. https://doi.org/10.1016/S0955-2219(02)00139-5
24. King S., French M., Bielefeld J., and Lanford W. - Fourier transform infrared spectroscopy investigation of chemical bonding in low-k a-SiC: H thin films, J. Non-Cryst. Solids **357** (15) (2011) 2970-2983. https://doi.org/10.1016/j.jnoncrysol.2011.04.001
25. Kien K. D. T., Tuan P. D., Okabe T., Minh D. Q., and Khai T. V. - Study on sintering process of woodceramics from the cashew nutshell waste, J. Ceram. Process. Res. **19** (6) (2018) 472-478.
26. Kien K. D. T., Minh D. Q., Minh H. N., and Nhi N. V. U. - Synthesis of TiO_2-SiO_2 from tetra-n-butyl orthotitanate and tetraethyl orthosilicate by the sol-gel method applied as a coating on the surface of ceramics, Ceramics–Silikáty **67** (1) (2023) 58-63. https://doi.org/10.13168/cs.2023.0002
27. Chiew Y. L. and Cheong K. Y. - A review on the synthesis of SiC from plant-based biomasses, Mater. Sci. Eng. B **176** (13) (2011) 951-964. https://doi.org/10.1016/j.mseb.2011.05.037
28. Fneich H., Vermillac M., Neuville D. R., Blanc W., and Mehdi A. - Highlighting of LaF3 reactivity with SiO_2 and GeO_2 at high temperature, Ceramics **5** (2) (2022) 182-200. https://doi.org/10.3390/ceramics5020016
29. Taylor N. W. and Lin C. Y. - Effect of various catalysts on conversion of quartz to cristobalite and tridymite at high temperatures, J. Am. Ceram. Soc. **24** (2) (1941) 57-63. https://doi.org/10.1111/j.1151-2916.1941.tb14821.x